Cement and Concrete Research 39 (2009) 182–194

Contents lists available at ScienceDirect

Cement and Concrete Research

journal homepage: http://ees.elsevier.com/CEMCON/default.asp

Concrete mixing kinetics by means of power measurement

B. Cazacliu *, N. Roquet

Laboratoire Central des Ponts et Chaussées, BP4129, 44341 Bouguenais Cedex, France

ARTICLE INFO

Article history:
Received 20 December 2007
Accepted 9 December 2008

Keywords:
Dispersion (A)
Microstructure (B)
Rheology (A)
Mixing

ABSTRACT

This paper introduces a new model for concrete mixing kinetics. The model defines five successive stages through which the mixture characteristics change. It is also shown that the time-variation of the mixer power consumption is a relevant tool to identify the transient stages of the mixture during mixing. In particular, it detects the instant when maximum cohesive paste occurs and identifies the fluidity time. The fluidity time is the instant when mixture turns to fresh concrete. In that sense, this transition time can be seen as an indicator of mixing difficulty for a given mixer. The influence of the mix-design and that of the liquid loading sequence on the mixing behavior are investigated; three sets of experiments are used for the assessment of the model. It is shown that one key parameter is the rheology of the mixture at the fluidity time.

1. Introduction

All concretes require mixing. A set of objective criteria for mixing process adjustments has become increasingly necessary, mainly as a result of the rising demand for self-compacting concrete. In-line measurements of the quality characteristics of mixed concrete are currently available (see, for example, [1–5]) in both central mixer or mixing truck systems. New types of in-mixer sensors, along with the improved processing of existing sensors, however are to be anticipated. These advances rely upon a better understanding of mixture evolution during the mixing process.

Concrete mixing mainly consists of dispersing constituents into the mixed volume and then having the mixture evolve from a wet granular state to a granular suspension microstructure. While some of the research regarding constituents' dispersion in concrete or cement paste has been described in the literature [4,6–12], less interest was given to the microstructural evolution during mixing.

Starting with concepts developed in the literature presented in Section 2, mainly concerning wet granulation processes [13], the present paper proposes in Section 3 an explanation of the mechanism of mixture evolution during concrete mixing. The proposed explanation also stem from a laboratory experiment detailed at the beginning of Section 3.

Once the mechanism is understood, mixer power consumption will be defined as an indicator of the mixture kinematics, as well as for various wet powder products whose mixture state is associated with the corresponding power consumption or torque [14]. Characteristic points (transition states) within the mixture evolution will then be established and detection methods using the power consumption will be proposed. Three examples described in Section 4 from laboratory and *in situ* tests will serve to display the trends in these characteristic mixture evolution points.

From a research point of view, the power measurement is utilized here to better understand the microstructural mixture evolution during mixing. From the industrial point of view, a better understanding of this mixing kinetics permits a better use of in-situ power measurements to control the process.

2. Literature review

Two domains, dedicated to wet granulation process and to cement based materials, have been perused. Therefore, a description of different microstructural wet granular states and their evolution during mixing is given. The correlation between the microstructure and the power consumption is then described.

2.1. Physical states of wet powder materials

Several descriptions of the physical state of a wet granular mixture can be found. The physical state is described as a function of the water to powder mass ratio (w/p), after adequate mixing. Among the references, Goldszal and Bousquet [15] describe the states of wet particles as a function of the amount of the moisture content in the following manner:

- at very low moisture content, individual particles create liquid bridges between one another, i.e. pendular state, and form clusters (reaching an average critical size);
- when the amount of liquid increases the interparticle space begins to be filled, i.e. funicular state;
- when the spaces are entirely filled by the liquid, the clusters are saturated, i.e. capillary state;

* Corresponding author.
E-mail address: bogdan.cazacliu@lcpc.fr (B. Cazacliu).

0008-8846/$ – see front matter © 2008 Elsevier Ltd. All rights reserved.
doi:10.1016/j.cemconres.2008.12.005

– then, the liquid is used to create liquid bridges between clusters; once this second porosity is completely filled by the liquid, a solid–liquid dispersion state is ultimately obtained.

Concerning the cement paste Lombois-Burger et al. [7] define the following:

– a low-cohesion, humid powder or a non-cohesive paste at very low w/p (typically inferior to 0.20);
– a cohesive paste that reflects light due to the formation of a liquid film on the surface, subdivided into a hard (with a w/p typically inferior to 0.28) and soft (w/p less than 0.32) pastes, undergoing respectively brittle and ductile fracture under tension; and
– a creamy paste (higher w/p values) that spontaneously fills a groove made by a spatula tip.

When analyzing the microstructure of cement paste, Yang and Jennings [16] observed agglomerates averaging 0.3 mm in size that did not rupture during mixing within a poorly-mixed cement paste. Inside these agglomerates, the particles were dry. The size and quantity of agglomerates drop significantly in a well-mixed paste. Williams et al. [8] associated the decrease in agglomerates size to the level of mixing shear.

2.2. Kinetics of liquid distribution

The kinetics of liquid distribution has been extensively analyzed during wet granulation processes. Carstensen et al. [17] suggested that the initial stage mixing of a liquid with a powder involves the production of liquid drops surrounded by powder.

Quite rapidly thereafter [18], the liquid distribution forms small granules with continued mixing. The formation of agglomerates has been termed “nucleation”.

Coarser granules containing solid, liquid and air are formed after short mixing times. Knight et al. [18] also suggested that granules gradually consolidate as they collide during subsequent mixing with other granules and the equipment surface.

Compaction squeezes gas out of the spaces between particles. Once the liquid has completely filled the interparticle space, further compaction conveys liquid to the surface of the granule and favors coalescence. These two primary stages of the granulation process lie within a sequence of three combined steps: i) wetting and nucleation, ii) consolidation and coalescence, and iii) attrition and breakage [13].

Once a granular suspension has been obtained, liquid distribution continues as a consequence of powder agglomerates dispersion. Agglomerate destruction, associated with a decrease in the power consumption [7], is analyzed by Jézéquel et Collin [9] by applying the dispersion kinetics of colored, cohesive, tracer particles that gradually disaggregate during stirring.

2.3. Influence of microstructure on the power consumption

Torque measurements of a progressively wetted powder system were used to characterize the mixture state after adequate mixing [19]. Power consumption of the mixing motor is an easy-to-implement alternative method for identifying the states described in 2.1 [14,20]. From the pendular state (at the starting point of operations) leading to the suspension, the variation in power consumption vs. liquid addition generates a sort of “signature” of the process, also known as the cohesion function [15], which can be described as follows:

Phase I As previously discussed (for instance in [21]), at low liquid content, moisture becomes absorbed by powder particles without the formation of any liquid bridges and power consumption does not increase.

Phase II Power consumption is observed to increase at a saturation rate of approximately 25% since liquid bridges form between the powder particles and the first granules.

Phase III The addition of liquid results in filling the interparticulate space and forming coarser granules; moreover, power consumption levels off with liquid content.

Phase IV Another marked increase in power consumption is observed at approximately 80% saturation, at which point large areas in the particulate system are completely filled with liquid. Power consumption rises and falls with liquid content before reaching a maximum when the liquid saturation equals 100%. Power consumption then decreases as the liquid becomes excessive and the system transitions into a state of suspension.

Some differences in the cohesion function profile may be noted during Phases II and III from one mixer to the next [21].

The fluctuation in time of the power consumption (called below “power fluctuation”) shows a similar evolution as the cohesion function. More specifically, increased power fluctuation is observed in Phases III and IV (see, for instance, the curves given in [14,22]). This particularity is sometimes utilized in order to improve process monitoring [23,24].

2.4. Concrete mixer power consumption

The cohesion function description started in the early seventies. Investigating the correlation between power consumption value and concrete flow characteristics has been tackled much earlier, but this truck remained mainly unexplored. In 1928, Loring and Purrington [25] first mentioned the idea of using power consumption to monitor the workability of concrete used in production. Several papers [26–33] and patents ([34], see also the list presented in [35]) followed. In the United States, the methods were mainly adapted to truck mixers, whereas in France the evolution in mixer motor power consumption during mixing (called the “wattmeter curve”) was extensively analyzed during the 1960s to characterize the batching process. Some of the key trends (see Fig. 1) have been summarized in [2], i.e.:

a. the increasing power during loading provides information on the loading system and automatic operations;
b. at a given loading sequence, the power peak depends on the mixer loading level;
c. the decrease in power is indicative of mixer homogenization efficiency;

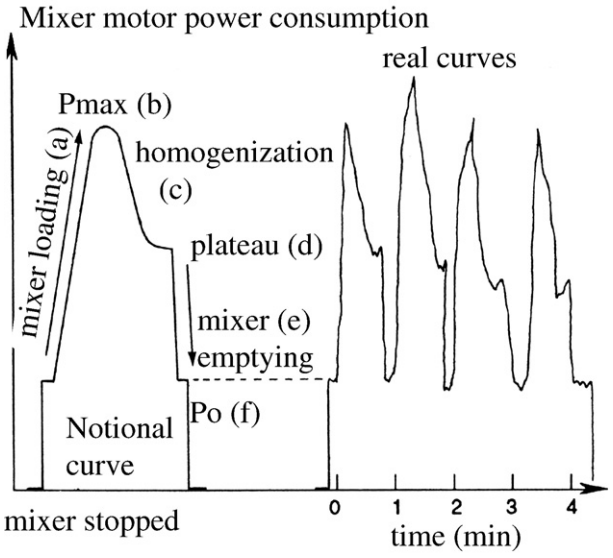

Fig. 1. Description of the power consumption evolution [2].

d. the stabilization power level is correlated with water content (at a constant proportioning of other constituents and loading sequencing) or, in certain limited cases, with slump measurements; the amplitude of variation in the plateau signal for similar batches measures the homogeneity in flow characteristics;
e. the decrease in power during emptying is a significant indicator of blade wear; and
f. the power level after emptying serves to detect if the mixer emptying step is complete.

These analyses are complex and data acquisition has not, for the time being, been able to associate the power curve with batch composition. Consequently, research interest waned halfway through the 1970s, and industrial applications were mainly restricted to certifying loading conditions and mixing time for a given batch. Interest was renewed during the 1990s [2,3,6,36–38], as advances in control and acquisition systems enabled the systematic surveying of power consumption measurements; however, with the exception of improved databases, industrial applications have not evolved from the previous simplified analyses.

3. Mixture evolution during concrete mixing

Concrete mixing kinematics have been highlighted for an ultra high performance self-compacting concrete (UHPSCC). The hard-to-mix nature of this concrete, which features a greatly expanded mixing time scale, facilitates both visual and power observations. The components are mixed in a 20-liter, twin-shaft laboratory mixer filled

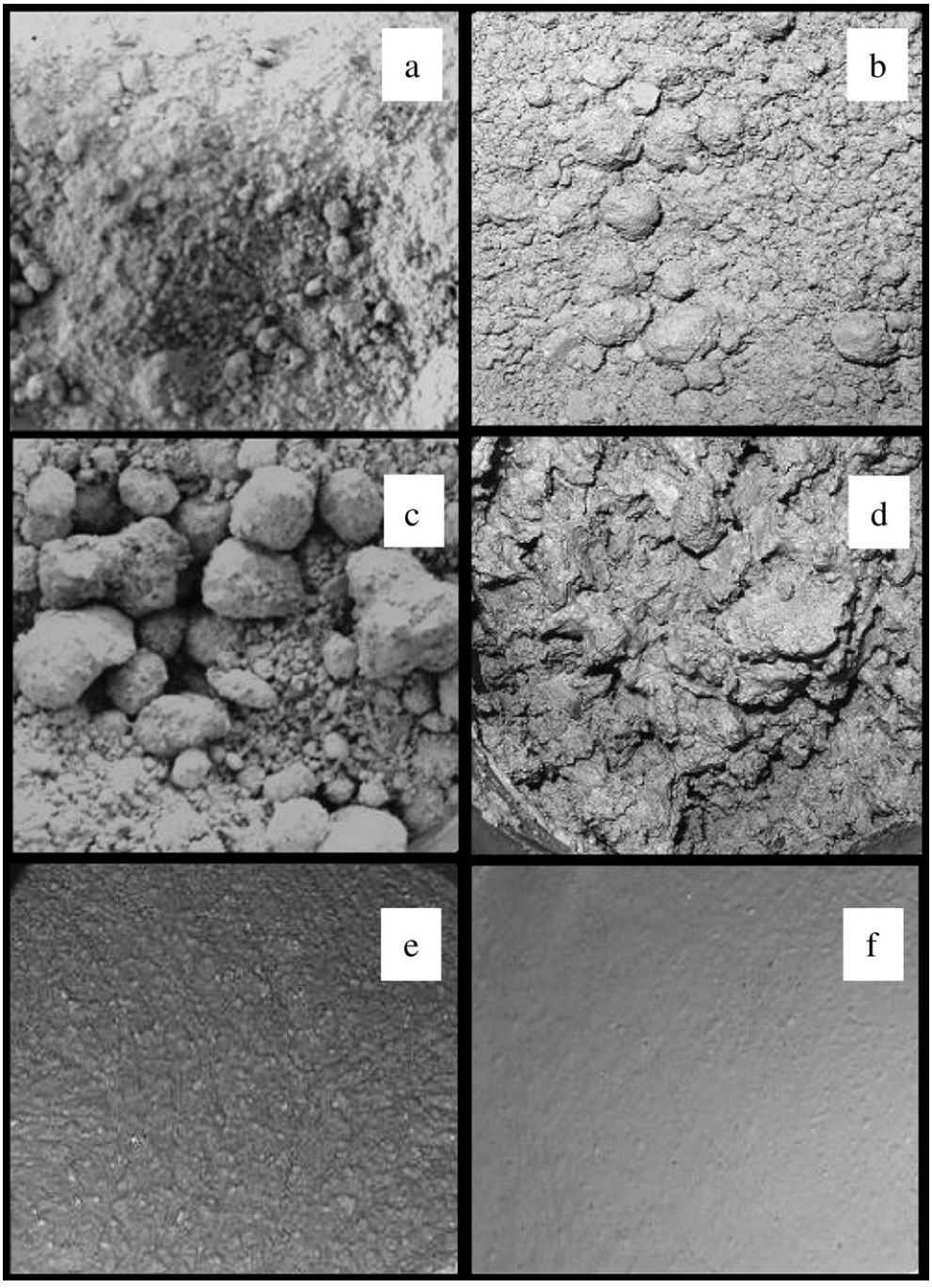

Fig. 2. Mixture evolution during the mixing of an ultra high performance SCC at a. 0′30, b. 1′30, c. 2′00, d. 3′00, e. 6′00 and e. 8′00 after the beginning of liquid loading.

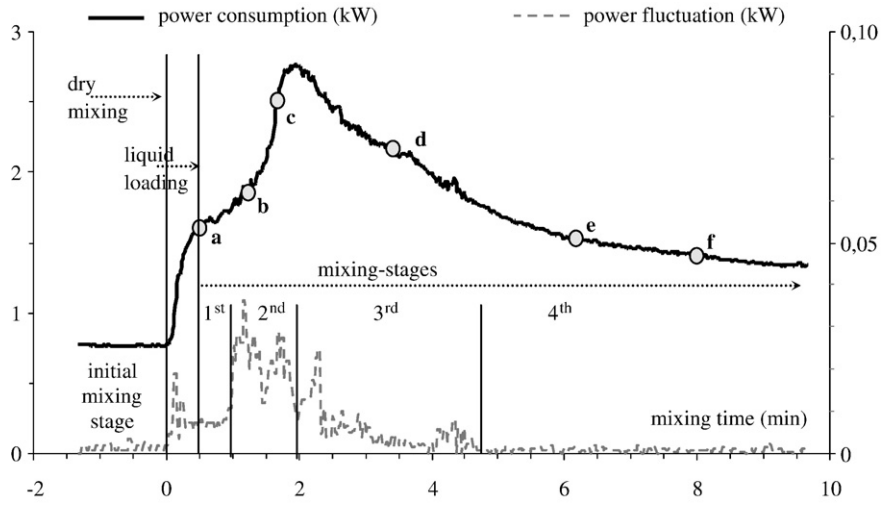

Fig. 3. Power consumption and its fluctuation evolution during the mixing of an ultra high performance SCC in a laboratory twin-shaft mixer; the points a–f refer to the Fig. 2a–f.

to a nominal level. The mix design is defined by: a water-to-fines ratio of 0.15, high-range water reducer admixture (HRWRA) proportioned at powder adsorption saturation (plateau of the adsorption isotherm), with powder composed of white cement (900 kg/m^3) and silica fume (300 kg/m^3), and the remaining solid particles composed of 0–1 mm sand. After 90 s of dry mixing of the solid components, premixed water and HRWRA are loaded at a constant flow rate during an additional 30 s. The origin of the mixing time is set at the beginning of liquid loading.

The mixture state at six different mixing times is shown in Fig. 2. The mixer power consumption measured during this test is given in Fig. 3, which also indicates the points corresponding to the six mixing states from Fig. 2. The filtered power consumption profile is associated with a measurement of power fluctuation vs. time. This fluctuation is measured herein by the difference between two successive power consumption measurements, in absolute value terms. The time interval between measurements is 0.1 s. The figure depicts the maximum of this difference during the 3 last seconds of measurement before indicated time.

Several mixing stages can be noted in Fig. 3. The dry mixing is characterized by constant power consumption and low power fluctuation. The liquid loading produces a sharp increase in both power consumption and power fluctuation. A few seconds after liquid loading, the mixture still reveals a dry appearance, although the formation of small granules can now be observed (Fig. 2a). These granules grow up as mixing progresses (Fig. 2b). During this 1st mixing-stage the power consumption and its fluctuation become stabilized but at higher levels than during the dry mixing. The 2nd mixing-stage is characterized by a second sharp rise in both power fluctuation and power consumption. The granules are wetted and conglomerate (Fig. 2c). Wet granules' coalescence is more visually discernible upon entering in the 3rd mixing-stage, in which the mixture appears to be already a paste with a "raspberry-like" shape (Fig. 2d). In the 3rd mixing-stage power consumption decreases yet large power fluctuations are still present. Once all volume has been transformed into a granular suspension (4th mixing-stage), the free surface of the mixture becomes smoother (Fig. 2e). At this particular mixing time, power fluctuation decreases rapidly and significantly while power consumption continues to decrease. The planer surface of the concrete however displays lumps whose size decreases as mixing continues, which generates a creamy appearance at the end of mixing (Fig. 2f).

Concrete mix design provides sufficient water to completely saturate the granular skeleton. Following sufficient mixing, the mixture attains a solid–liquid dispersion state (granular paste). At an intermediate mixing time, the mixture heterogeneity and transitory microstructure generate domains of unsaturated granular material. Thus, one can deduce that the mixture develops different states presented in Section 2:

- dry solid particles;
- granules with the surface dry;
- granules with the surface wetted;
- granular suspension containing groups of powder elements shared by a hydrate membrane; and,
- granular suspension with dispersed solid components.

The energy dissipated by mixture flow has frictional origin in dry solid particles and dry granules state, cohesive nature for the wetted granules state and is generated mostly by viscous effects in the granular suspension.

In taking into account the above descriptions of the power consumption evolution with mixing time, an outline of the wet powder evolution during mixing can be suggested below.

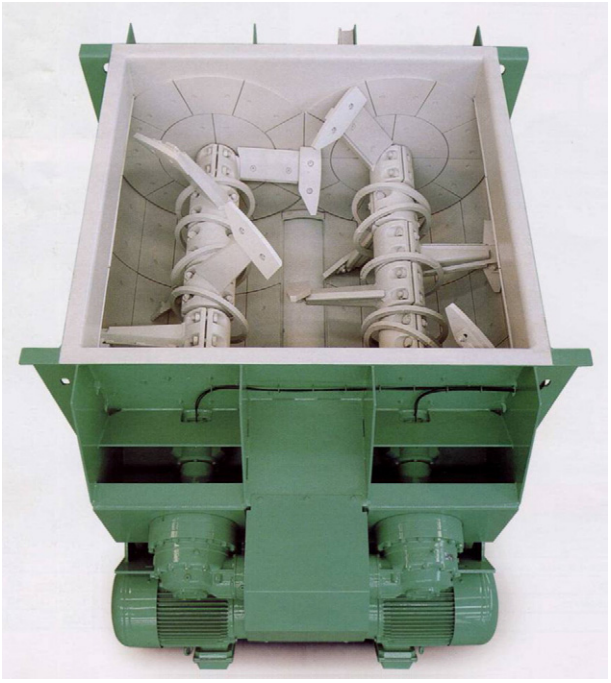

Fig. 4. 500-liters twin-shaft mixer used for batching the UHPSCC.

Table 1
Batch characteristics for UHPSCC production in 500-liters twin screw mixer

Batch	I01	I02	I04	I05	I07	I08	I09	I10	I11
Filling level	51%	49%	51%	51%	51%	52%	52%	53%	51%
Premixed solid components	New	New	New	New	New	New	New	New	Aged
Water dosage (kg/m3)	215	210	207	200	190	190	195	195	205
HRWRA delay (min)	2	2	1	1	1	3	1	2	2
Time corresponding to maximum cohesion (s)	51	63	78	73	107	77	93	89	257
Time corresponding to fluidity (s)	86	115	127	120	159	129	154	145	296

3.1. Dry mixing: Agglomerates formation

In dry components, groups of powder elements naturally form. These microstructural elements are referred to as agglomerates. The voids between agglomerate particles create the agglomerate porosity.

3.2. Liquid dispersion: Granules formation

The liquid injected into the powder spreads into droplets, which are then coated by fine particles and agglomerates, hence forming granules. A number of liquid bridges are formed and yield an increase in power consumption. Heterogeneities in the liquid distribution also stimulate increased power fluctuation.

3.3. 1st mixing-stage: Granules growth

Granules consolidate by shearing. The liquid squeezed out serves to glue the dry powder which is still present in the mixture and enlarge the granules. The granules increase yet remain dry at the surface. The power dissipation is mainly frictional with no reason to significantly increase. The dry powder progressively consumes to form granules.

3.4. 2nd mixing-stage: Granules coalescence

When dry powder is consumed, the liquid released by granule consolidation gradually wets free surfaces. Cohesion strengthens with the quantity of liquid bridges formed and produces a sizable increase in power consumption. Heterogeneity between the wet and still dry granules generates high power fluctuations over time. When power consumption reaches a peak value, wet granules cover almost the entire mixed volume. The mixture becomes a “hard paste” displaying a “raspberry-like shape”, as characterized by a high consistency that generates a very irregular free surface.

3.5. 3rd mixing-stage: Granules dissolution

Once all free surfaces have been soaked, liquid which continues to exit from the sheared granules gradually fills the voids between granules and/or coarser grains (i.e. second porosity). Cohesion decreases as granular suspension is created in some regions of the mixer and corresponding liquid bridges vanish. Consequently, power consumption decreases, although large power fluctuations remain present as a result of heterogeneities between saturated and unsaturated sheared zones.

3.6. 4th mixing-stage: Agglomerate dispersion

Once the second porosity has been completely filled with liquid, the granular suspension is complete. The granules dissolve but the granular fluid still contains a large quantity of agglomerates (Fig. 2d) shared by a hydrate membrane [8,16]; these agglomerates possess flow-inhibiting properties [39]. When suspension is first formed, the fluid typically is just barely sufficient to fill voids between the tightened particles (both aggregates and agglomerates). The mixture however displays a fluid-like behavior since a sizable quantity of the energy needed to achieve flow is used to disperse water through the granular skeleton. Yet plastic behavior also proves important given that interparticle distance is small. As dispersion proceeds and agglomerates are destroyed, the effective solid volume fraction decreases. The fine elements freed are introduced between loosening larger particles [40] and lend a creamy appearance to the concrete (Fig. 2f). The viscosity and the yield stress of cement paste consequently decreases, thereby inciting a decrease in power consumption with a trend towards stabilization. The mixture is now homogenously a granular suspension, and this serves to significantly reduce power fluctuations.

From a practical standpoint, power consumption allows determining different transitory states of mixing, i.e.:

- Liquid loading is associated with an increase in power consumption. This increase levels off soon after the liquid has finished loading.
- Dry powder is consumed when major power fluctuations occur.
- Hard paste is formed throughout the mixer once the peak power has been reached. This point is referred to as the “maximum cohesion point”.
- The transition to a granular suspension (soft paste) corresponds to a large decrease in power fluctuation. This point is referred to as the “fluidity point”.
- The concrete obtains optimal flowability when the power rate (the first differential with time) becomes negligible from a practical point of view.

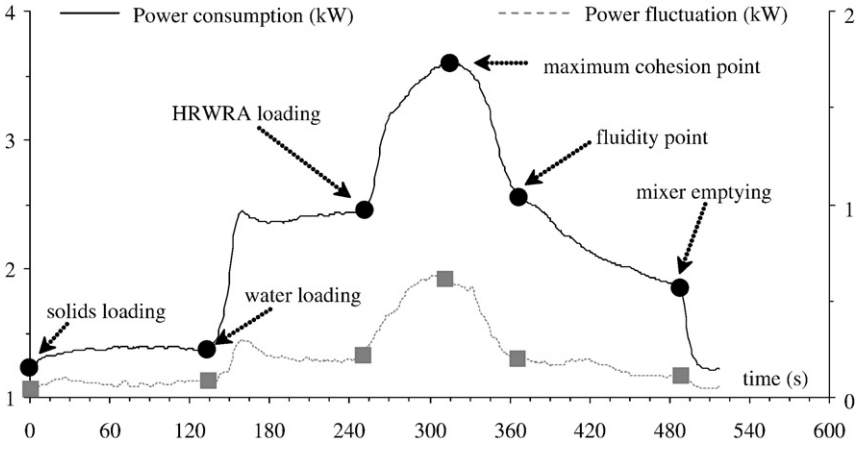

Fig. 5. Power consumption and power fluctuation time-evolution for batch I02.

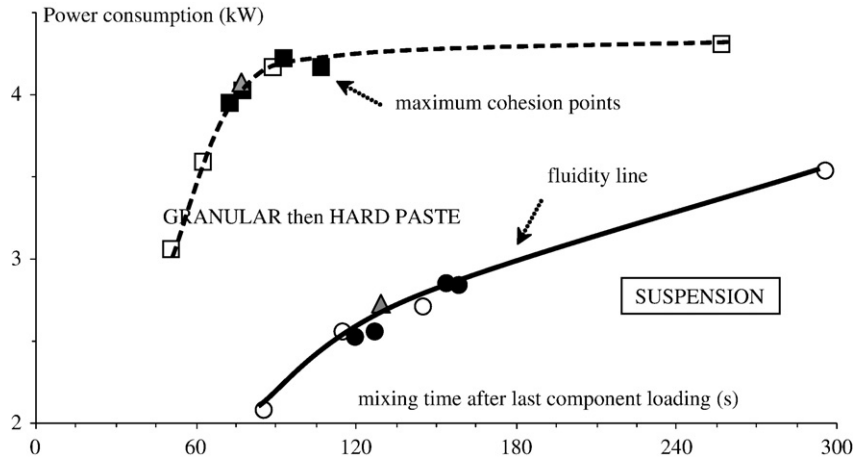

Fig. 6. The location of fluidity and maximum cohesion points for the nine batches; black dots corresponds to batches with 1 min delay between the water and HRWRA loading, white dots to 2 min delay and triangles to 3 min.

Among these concepts, the fluidity point is particularly important in practical terms since it determines the time at which the concrete arises from the mixture.

4. Experimental results

Results from three studies conduct by the LCPC are presented here to support the concepts above.

4.1. Mixing of UHPSCC

The ultra high performance SCC described above was produced at the LCPC real scale concrete plant, by using a 500-liter twin-shaft mixer (Fig. 4). Filling level during batches is around 50% to avoid over-charge in power consumption of the mixing motor. Slight fluctuations in the filling level are however observed.

The nine manufactured batches (Table 1) have fixed mix-design except for the water content which is varied from 190 to 215 l/m^3. The loading sequence is as follows:

- dry mixing of all solid components for 1 min;
- water is loaded during 15 s;
- HRWRA is loaded 1, 2 or 3 min after the beginning of water loading (the delay is indicated for each batch in Table 1); the HRWRA loading lasts 7 s.

When analyzing a typical power consumption profile with respect with time (for instance batch I02, Fig. 5) one can observe a slight increase during premix loading. Sharp increases during both liquid loadings (water and HRWRA) follow to obtain a maximum power point (maximum cohesion point). The power consumption then decreases. The power fluctuation has similar evolution, but permits much easier detection of the fluidity point.

For each of the nine batches, Fig. 6 shows both the maximum cohesion and the fluidity points with respect with time measured from the loading of last component (in this case the HRWRA). The corresponding master curves are mainly bi-linear (two linear segments). Concerning the fluidity line, an acceptable fitting is obtained by a logarithmic evolution of fluidity power in time.

The fluidity line divides the power consumption to time chart into two domains. After the fluidity line the mixture is a granular suspension, already having the fresh concrete appearance. Prior to the fluidity line the mixture is a wet granular material then a hard paste, with “raspberry-like” surface.

4.2. Mixing of ready mix SCC in industrial plant

This experiment is carried out in Couvrot batching plant in the SBP Samer factory equipped with a 1.5 m^3 planetary mixer. The mixing system is described in Fig. 7. The filling cycle is as follows: simultaneous introduction of aggregates (natural moisture) and fines (cement and filler) then introduction of liquid components after about 10 s. The mixing time with all components is at least 55 s before discharging in a truck mixer.

The SCC mix design analyzed for the experiment has a sand to gravel ratio of 1.05, 380 kg/m^3 of fine elements (75% of cement and 25% of filler), HRWRA (4.7 kg — corresponding to the maximum absorption proportioning). Crushed coarse aggregates from two size fractions, 6/12 mm and 4/20 mm, were used. The 0/4 sand has about 8% of fines content. The cement was a CEM I 52.5 R. Twelve batches of various water content, from 168 to 203 l/m^3, were produced. Total water content was used here to compare the batches as these mixtures had the same amount of water absorbed (constant aggregates content). The moisture of sand was measured for each batch through a microwave moisture meter, coarse aggregates moisture being considered constant during all the day. The water content was verified by “in-mixer” measurements (Fig. 7). The precision of the indication of batch water contents is better

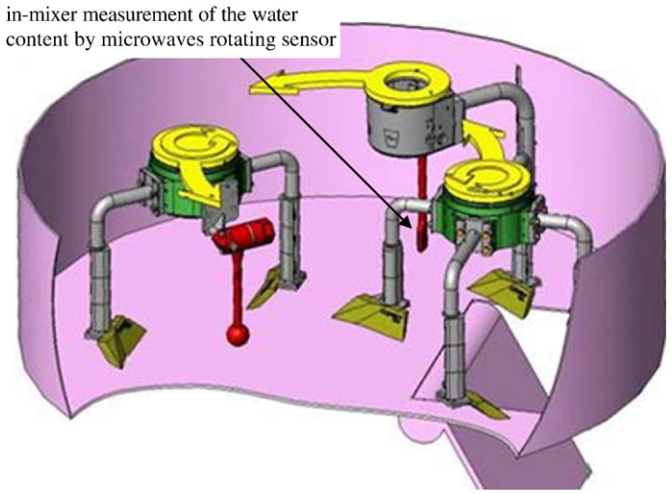

Fig. 7. Planetary mixer of the Couvrot batching plant with “in-mixer” moisture sensor (schema furnished by Couvrot).

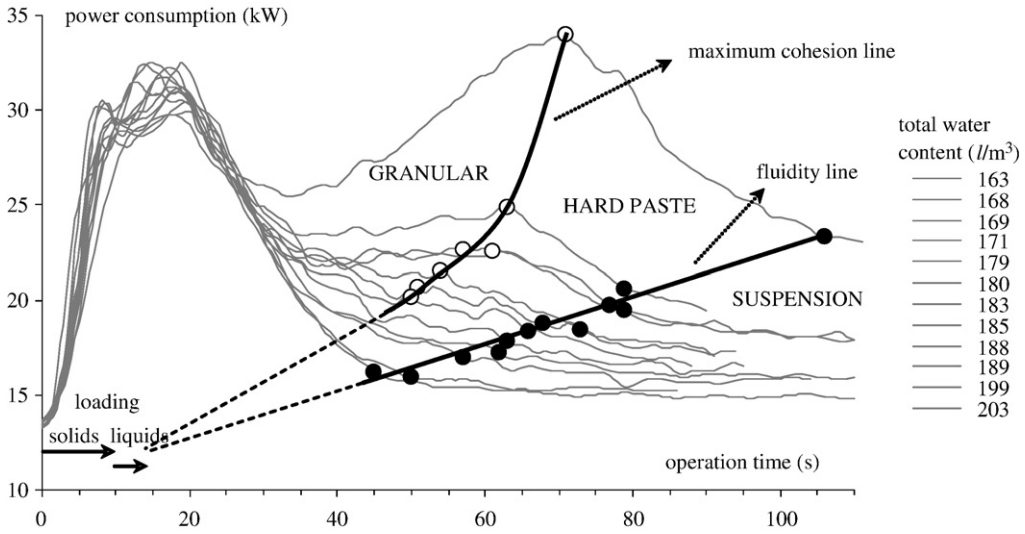

Fig. 8. Power consumption vs. time charts for the twelve batches on Couvrot plant.

then 2 l/m^3. The slump flow laid between 490 and 700 mm. The few concretes with a slump flow lower than 600 mm were those where water proportioning had been voluntarily reduced.

For the twelve batches, Fig. 8 shows the experimental mixer power consumption evolution with respect to time. The indicated operation time includes the loading of the mixer. The loading sequence generates an increase in power consumption. Once the mixer completely charged, the power consumption has a first peak. Constituents' loading is followed by a second power peak for batches with lower water dosage. The power then decreases and a relative stabilization occurs.

The data acquisition being of only one measurement per second, fluidity points are harder to detect by a power fluctuation analysis. However, the example in Fig. 9 corresponding to the batch with 169 l/m^3 of total water shows that the method is still discriminate. The figure also represents the second peak of the power curve. Complementary analysis based on three "in-mixer" sensors [1] confirms that the second power peak corresponds to the maximum cohesion point.

The fluidity and maximum cohesion points may be fitted respectively by a fluidity line and a maximum cohesion line (Fig. 8). The concavity of the maximum cohesion line is changed compared to the UHPSCC case mixed in twin-shaft mixer. It may be assumed that the two lines intersect at the end of liquid loading, in the hypothetic case of a very large amount of added water (the mixture became directly a suspension without a hard paste stage). So, the power to time chart is divided in three domains. As previously indicated, the state of mixture before the maximum cohesion line is mostly wet granular; between the two characteristic lines the mixture is a hard paste and becomes a granular fluid after the fluidity line.

4.3. Mixing of different concrete mix-designs in a same mixer

Sixty concrete mix-designs corresponding to High Performance Concrete, Self Compacting Concrete or ordinary concrete were produced in the LCPC real scale mixing station. Forty-eight of these tests were already presented in [38]. A different analysis of the power consumption profile in time is given here.

Concrete is batched in a 330-litre Couvrot planetary mixer at its nominal filling level. Solid components were loaded during first 15 to 18 s of operation time. Added water premixed with the HRWRA followed during about 6 s. The power consumption was measured every second. The fluctuation of the power curve was assessed here by calculating the standard deviation on 21 consecutive power measurements (10 s before and 10 s after a given mixing time). The mixing time was chosen long, about 10 min, for the purpose of this study. This long mixing time permits an improved detection of the fluidity point and a fitting of the mixing behavior after the fluidity time.

Two levels of fine particles content were chosen, 425 and 550 kg/m^3, respectively. In all batches these fine particles mainly consisted of cement, together with some silica fume (for HPC) or limestone filler (for SCC). The cement was Lafarge, 52.5 CP2 from Saint Pierre Lacour or

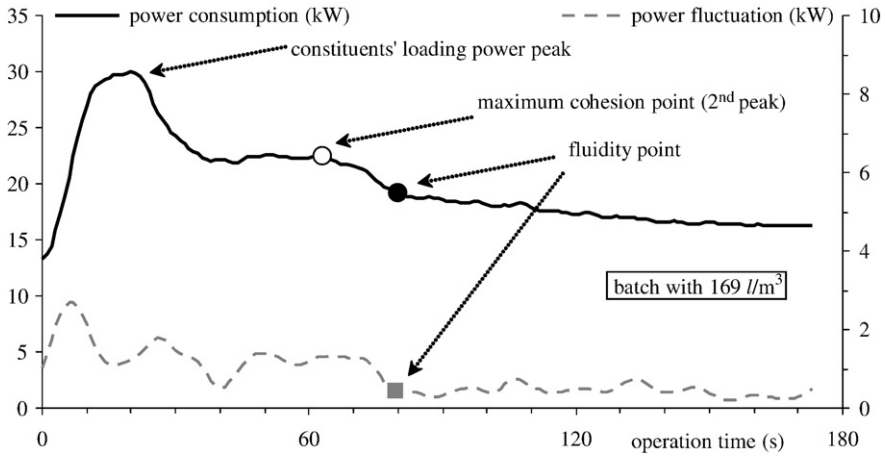

Fig. 9. Power consumption and power fluctuation with time for batch with 169 l/m^3 on Couvrot batching plant.

52.5R from Le Havre. Two types of superplasticizer were alternatively used at 40% or 100% of the saturation threshold: polycarboxylic-type (MBT Glenium 27) and melamine-type (Chryso GT). Other HRWRA contents were tested. Cohesion agent was employed for some SCC mixes. Coarse aggregates were crushed materials from two size fractions: 5/12.5 mm and 10/16 mm. The natural river sand was graded from 80 µm to 4 mm. All aggregates were from Lafarge — Les Pontreaux. For most batches the packing density was maximized by using a sand/gravel ratio of 0.85. Other sand to gravel ratios (from 0.48 to 2) were also tested. The mixtures composition is given in Table 2.

Concrete fluidity after mixing is characterized by slump or slump-flow tests and by the rheology of the final mixture. The rheology is given as a Bingham model (Table 1), measured using a concrete rheometer (the BTRheom [41]). Mixtures covers (even exceeds) usual concrete rheology domains, with viscosity from very low up to 250 Pa s and yield stress from 100 to 2000 Pa.

Table 2
Formulation and rheology of mixtures

Test name	Type of concrete	Cement (kg/m^3)	Water/powder	Type of HRWRA[a]	Admix./cement	F or SF[b]/cement	Sand/gravel	Slump (mm)	μ (Pa s)	τ_o (Pa)	*Re**	Coh. agent
C01	HPC	423	0.48	PC	0.12%		0.85	235	23	385	24.9	no
C02	HPC	392	0.53	PC	0.12%	SF 9%	0.86	200	9	533	24.0	no
C03	HPC	393	0.52	PC	0.12%	SF 9%	0.86	200	4	480	28.5	no
C04	HPC	393	0.53	PC	0.11%	SF 9%	0.85	250	4	284	46.0	no
C05	HPC	420	0.43	PC	0.30%		0.86	245	76	397	13.7	no
C06	HPC	390	0.49	PC	0.30%	SF 9%	0.86	200	5	407	32.6	no
C07	HPC	392	0.49	PC	0.30%	SF 9%	0.84	200	10	603	21.2	no
C08	HPC	392	0.45	PC	0.28%	SF 9%	0.86	210	11	424	28.2	no
C09	SCC	426	0.51	PC	0.30%		0.84		19	366	27.5	yes
C10	SCC	429	0.51	PC	0.30%		0.88					yes
C11	SCC	296	0.47	PC	0.30%	F 43%	0.85		25	304	27.9	yes
C12	HPC	422	0.44	PC	0.30%		0.85	210	108	401	10.8	no
C13	HPC	553	0.40	PC	0.12%		0.87	250	18	162	45.6	no
C14	HPC	502	0.45	PC	0.12%	SF 9%	0.84	200	5	588	23.2	no
C15	HPC	511	0.45	PC	0.12%	SF 9%	0.82	210	4	700	20.0	no
C16	HPC	508	0.44	PC	0.11%	SF 9%	0.84	260	11	291	37.8	no
C17	HPC	548	0.35	PC	0.30%		0.86	170	99	830	8.6	no
C18	HPC	551	0.34	PC	0.30%		0.86					no
C19	HPC	502	0.41	PC	0.30%	SF 9%	0.84	200	6	618	21.9	no
C20	HPC	504	0.41	PC	0.30%	SF 9%	0.84	190	11	676	19.0	no
C21	HPC	506	0.35	PC	0.30%	SF 9%	0.86					no
C22	HPC	505	0.38	PC	0.28%	SF 9%	0.85	230	43	492	16.8	no
C23	SCC	550	0.41	PC	0.30%		0.85		16	467	24.1	no
C24	SCC	545	0.43	PC	0.30%		0.85					no
C25	SCC	383	0.41	PC	0.30%	F 43%	0.84		30	127	37.3	no
C26	HPC	420	0.46	M	0.49%		0.84	230	52	326	18.6	no
C27	HPC	423	0.39	M	0.31%		0.85					no
C28	HPC	390	0.46	M	0.49%	SF 9%	0.85	200	32	554	17.5	no
C29	HPC	391	0.46	M	0.49%	SF 9%	0.86	200	24	550	19.3	no
C30	HPC	392	0.53	M	0.49%	SF 9%	0.84					no
C31	HPC	422	0.42	M	1.22%		0.85	200	60	592	13.1	no
C32	HPC	387	0.41	M	1.23%	SF 9%	0.86	200	60	534	13.8	no
C33	HPC	388	0.41	M	1.23%	SF 9%	0.85	190	58	530	14.1	no
C34	SCC	422	0.46	M	1.23%		0.86		24	85	49.2	yes
C35	SCC	296	0.43	M	1.23%	F 43%	0.85		43	227	24.1	no
C36	HPC	548	0.38	M	0.49%		0.86	230	52	406	16.9	no
C37	HPC	503	0.39	M	0.49%		0.85	230	17	487	23.0	no
C38	HPC	503	0.39	M	0.49%		0.86	210	14	508	23.2	no
C39	HPC	545	0.35	M	1.23%		0.85	200	95	671	9.7	no
C40	HPC	497	0.37	M	1.23%		0.83	200	46	644	14.0	no
C41	HPC	501	0.33	M	1.23%		0.85	150	80	1057	8.3	no
C42	SCC	544	0.40	M	1.23%		0.85		18	197	41.2	no
C43	SCC	382	0.37	M	1.23%	F 43%	0.86		56	269	19.2	no
C44	SCC	381	0.39	M	1.23%	F 43%	0.86					no
C45	–	431	0.40	PC	0.29%		0.56	90	236	1679	3.9	no
C46	–	425	0.37	M	1.23%		0.57	90	215	1913	3.8	no
C47	–	423	0.42	M	1.23%		0.56	210	170	410	7.6	no
C48	BO[c]	291	0.51			F 26%	0.52	140	87	930	8.6	no
C49	BO[c]	300	0.46			F 26%	0.50	110				no
C50	HPC	562	0.34	PC	0.12%	F 6%	0.54	220	122	327	10.4	no
C51	HPC	589	0.32	PC	0.30%		0.66	250	92	330	12.8	no
C52	HPC	587	0.32	PC	0.30%		0.68					no
C53	HPC	607	0.27	PC	0.12%	SF 10%	0.55	110	40	1352	8.6	no
C54	HPC	525	0.30	PC	0.30%	SF 10%	1.26	200	62	565	13.2	no
C55	HPC	450	0.34	PC	0.38%	F 11%	0.49	210	219	562	5.9	no
C56	HPC	448	0.34	PC	0.38%	F 12%	0.48					no
C57	HPC	453	0.33	PC	0.30%	F 11%	0.48					no
C58	HPC	451	0.34	PC	0.30%	F 11%	0.49					no
C59	HPC	434	0.33	PC	0.33%	SF 10%	0.99	190	141	613	7.9	no
C60	SCC	386	0.33	PC	0.50%	F 53%	2.01		103	269	12.4	yes

[a] Type of admixture: PC — polycarboxylic and M — melamine.
[b] (F) filler or (SF) silica fume.
[c] BO — ordinary concrete.

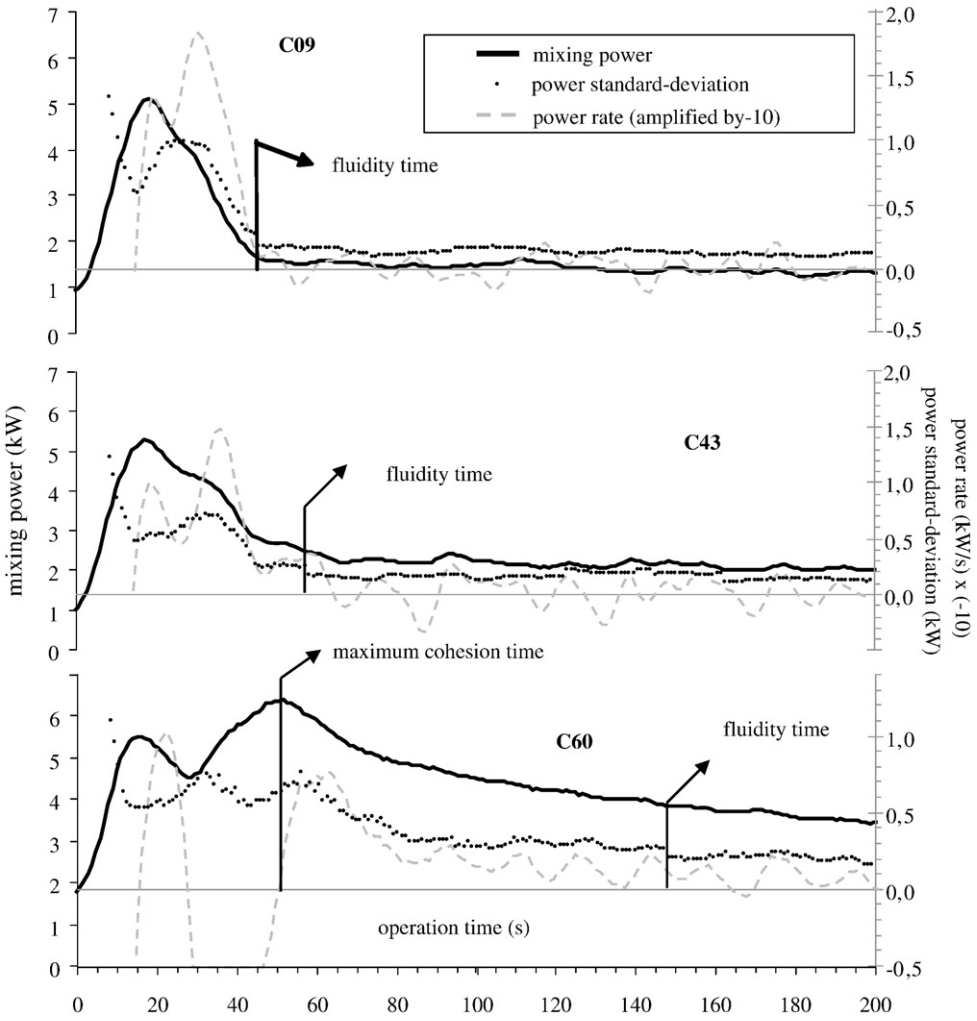

Fig. 10. Power consumption evolution with respect to time profile for mixtures C09, C43 and C60, power fluctuation and power rate.

Fig. 10 gives three of the obtained power consumption profiles with respect to time. The power fluctuation and the power rate profiles are also indicated. Between the three tests, the concrete C09 needs the shortest time to obtain fluidity. For this concrete the fluidity point corresponds to an angular point of the power consumption function with respect to time (sudden decrease in first derivative of the power consumption evolution over time). Thus, the angular point becomes a practical way to detect the fluidity time. However, for harder-to-mix concrete (in the sense that the mixing time needed to obtain fluidity is longer, i.e. C43 and C60 in Fig. 10) the angular point is not any longer observed. The fluidity time is better identified by observing the stabilization of the power fluctuation at a low level. The power fluctuation stands a better technique to detect the fluidity time, even if the method of identification may be improved.

Some concretes in these experiments also develop a maximum cohesion point. In particular, a second power peak is observed for concrete needing longer mixing time to obtain fluidity (concrete C60 in Fig. 10). A maximum cohesion point may be estimated for other

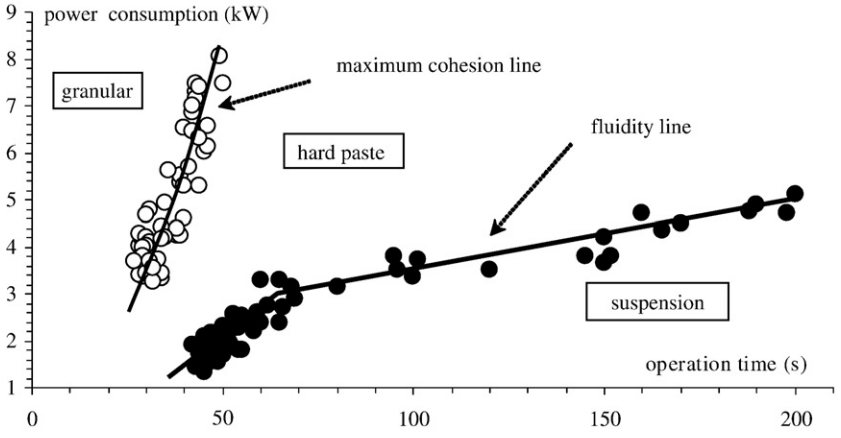

Fig. 11. Fluidity points and maximum cohesion points for 330-litre planetary mixer and various mix-designs.

mix-designs, as is the case of concrete C43 in Fig. 10. Both maximum cohesion and fluidity points for different mix-designs may be fitted by a fluidity line and a maximum cohesion line, respectively (Fig. 11).

5. Discussion

5.1. Influence of mix-design on fluidity line

During the mixing of Ultra-High Performance Self-Compacting Concrete (first set of experiments presented in the Section 4.1) data in Fig. 6 and Table 1 show that the fluidity points are positioned on the fluidity line approximately in the decreasing order with respect to the water dosage. The batch I11, corresponding to the longest mixing time to obtain fluidity, is a significant exception as it has a relatively high water content. This batch is an exception most probably because of different delivery of premixed solid components, with a different composition in the granularity of fine elements. It can be supposed that the position on the fluidity line is more related to the concrete flowability in the batch than to the water content alone.

As shown in the Fig. 12, the fluidity points are also located on the fluidity line in the decreasing order of the water content in the second set of experiments (mixing of the Self-Compacting in Couvrot plant, presented in the Section 4.2). During these tests, the other mix-design parameters were held constant. After calibration, the fluidity power may then be considered as an indication of the water content in the batch. As shown in [1], the standard deviation of the water content determined by using the fluidity power is of 2 l/m^3. This precision is more than two times better than a classic utilization of the power consumption to estimate the water content (in well calibrated measurement systems [42]).

At nominal water content (185 l/m^3) the mixing time of this Self-Compacting Concrete in the planetary mixer is reasonably short. However, the results presented here show that manufacture fluctuation in water content, sometimes larger then 15 l/m^3, may result in batches needing more time to mix. The good understanding of the power consumption evolution may help to give a fast answer, at an early stage of mixing, to these production problems.

The location on the fluidity line in function of the concrete composition is more thoroughly discussed using the third set of experiments (mixing of different mix-designs in a Couvrot 330-litres mixer, Section 4.3). It will be shown above that the time needed to obtain fluidity depends on the mixed concrete rheology. For this purpose the apparent Reynolds number at fluidity time, Re_f* is first introduced.

The apparent Reynolds number, Re* is defined as follows:

$$Re^* = \frac{\rho \Omega L^2}{\mu^*} \tag{1}$$

where ρ the specific gravity of the mixture, Ω the main angular velocity of the mixer, L a conventional length taken here the horizontal (largest) length of the blade, and μ* the mean apparent viscosity defined by using the measured viscosity μ and yield stress τ_o of the concrete at the end of mixing, and considering that an averaged shear rate in the mixed volume $\langle\dot{\gamma}\rangle$ exists:

$$\mu^* = \mu + \frac{\tau_o}{\langle\dot{\gamma}\rangle.} \tag{2}$$

It may be shown by fitting the experimental data [43] that for the given mixer, the apparent Reynolds number is proportional to the inverse of a Newton number, Ne:

$$Ne = \frac{P - P^*}{\rho \Omega^3 V L^2} \tag{3}$$

where P is the power consumption at a given mixing time, V is the mixed volume and P* a constant friction power.

The obtained relation:

$$NeRe^* = K_p \tag{4}$$

is equivalent to the expression deduced in [6]:

$$P = P^* + C_m \langle\dot{\gamma}\rangle (\mu \langle\dot{\gamma}\rangle + \tau_o) \tag{5}$$

if the Metzner and Otto [44] hypothesis is admitted for Bingham fluids:

$$\langle\dot{\gamma}\rangle = K_s \Omega \tag{6}$$

A mixer constant K_p equal to 12.8 is fitted by using the measured concrete rheology (Table 2) and power consumption at the end of mixing for respective batches. The relation (4) is *a priori* valid for all the states of the concrete into the mixer when mixture is already fluid. The apparent Reynolds number at fluidity time, Re_f*, is thus calculated by using the power corresponding to the fluidity point in relations (3) and (4).

The evolution indicated in the Fig. 13 shows that the time needed to obtain a concrete from the mixture decreases with the apparent Reynolds number at fluidity time. In other words, a higher level of rheological parameters (viscosity and/or yield stress) implies that

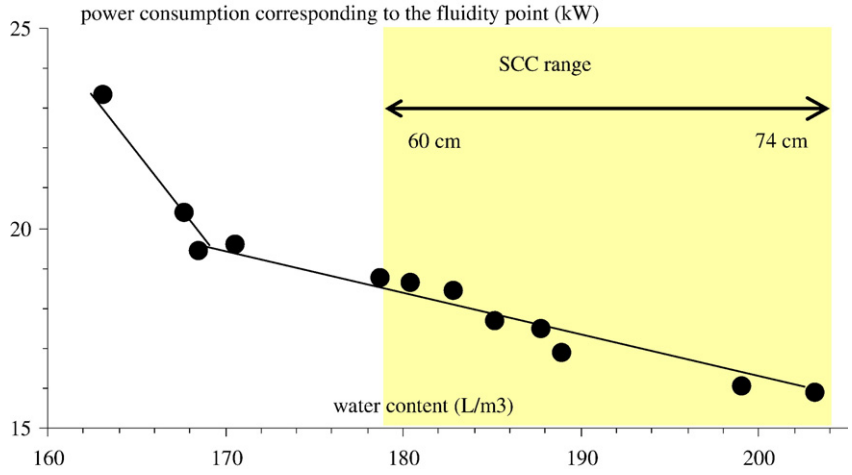

Fig. 12. Correlation between the power consumption corresponding to fluidity point and the water content for batches on Couvrot plant.

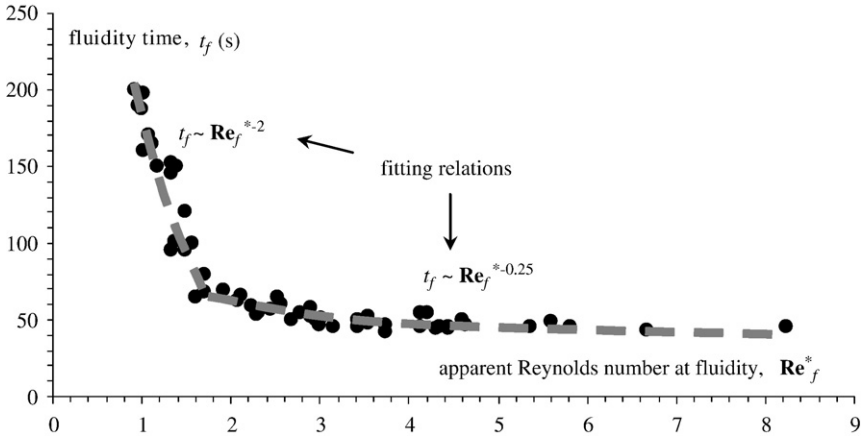

Fig. 13. Fluidity time (time needed to obtain a fluid mixture) evolution with concrete rheology.

longer time is needed to obtain fluidity. However, a Self-Compacting Concrete may be harder to mix than an ordinary concrete even if Self-Compacting Concrete has improved flowability when compared with an ordinary concrete, after adequate mixing time. It should however be remembered that the mixing behaviour depends on the value of the rheological parameters at the moment when the fluidity is obtained and, generally, the apparent viscosity is higher for the Self-Compacting Concrete than for the ordinary concrete when the mixture first transforms in a granular suspension.

A second discussion may be of interest. The apparent Reynolds number at fluidity time also depends on the mixer, through the averaged shear rate in the mixed volume. The order of mixing difficulty for several concrete mix-designs may change at different mixing speeds or in mixers with different geometry (i.e. when comparing high viscosity and low yield stress concrete, on the one side, with low viscosity and high yield stress concrete, on the other side).

Two mixing regimes may be observed by analyzing the data in Fig. 13: the fluidity time increases slower with Re_f* for high Re_f* concrete (i.e. low viscosity and low yield stress concrete at the fluidity point) than for low Re_f*. The two mixing regimes correspond to two domains in the viscosity vs. yield stress chart (Fig. 14). The chart displays the "easy-to-mix concrete" (high Re_f*) and "hard-to-mix concrete" (low Re_f*) domains separated by a linear border.

The angular point of the fluidity line may then be considered to characterize the mixer. It gives the limit (maximum) concrete rheology which keeps the mixing efficient in the given mixer. This concept applies for the two types of mixer discussed here: the twin shaft mixing system (Fig. 4) described in the Section 4.1 and the planetary mixing system (Fig. 7) which is described in the Sections 4.2 and 4.3 and tested in two different sizes: 1.5 m^3 and 0.33 m^3, respectively. The concept should hopefully be relevant for other mixers (including drums or truck mounted mixers).

5.2. Liquid loading influence on the fluidity line

The maximum cohesion and fluidity lines were defined in this paper by using the time scale measured from the last component loading. During the mixing of Ultra-High Performance Self-Compacting Concrete (experiments presented in Section 4.1) the delay between water and HRWRA loading has no influence on the maximum cohesion and fluidity lines (Fig. 6). During the third set of experiments, for some tests, premixed water and HRWRA loading were delayed with up to 20 s. Again, the effect of these delays on the maximum cohesion and fluidity lines (Fig. 11) is negligible. Consequently, it may be suggested that the liquid loading sequence into the solid components has no significant influence on the time and power corresponding to the maximum cohesion and to the fluidity points. More research is however needed to confirm this hypothesis.

5.3. Global trends of fluidity and maximum cohesion lines

The maximum cohesion and fluidity lines have similarities in the three set of experiments (Figs. 6, 8 and 11):

– the fluidity line is linear or bi-linear with lower slope for high rheology regime;

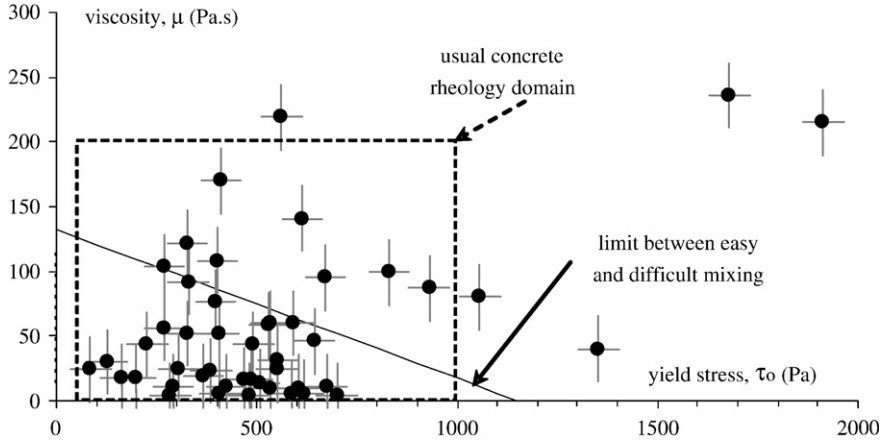

Fig. 14. Rheology domain of tested mix-designs; the BTRheom measurement uncertainty of rheological parameters is indicated by vertical and horizontal bars.

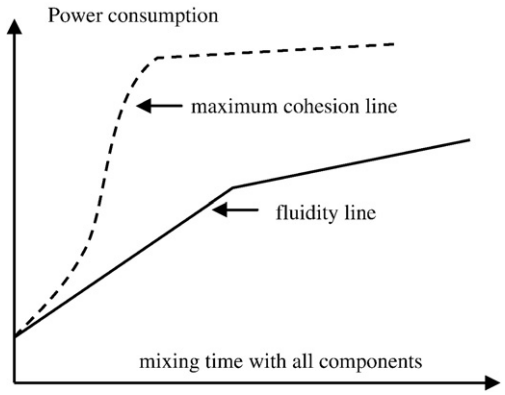

Fig. 15. Attempt of schematic representation of the maximum cohesion and fluidity lines trends.

– the maximum cohesion power increases much faster than the fluidity power for when fluidity time becomes longer.

Some important differences are equally observed. Nevertheless, it should be noted that the experimental conditions differ in the three examples. Three different mixers are used – 0.5 m^3 twin-shaft mixer, 0.33 m^3 and 1.5 m^3 planetary mixers – with respectively different range of water to powder ratio tested – from 0.14 to 0.16, from 0.30 to 0.53 and from 0.39 to 0.48. As shown in Section 5.1, the water to powder ratio is a key factor in the mixing behavior as it largely influences concrete rheology. Thus, it may be supposed that:

– Fig. 8 presents a part of the maximum cohesion and fluidity lines corresponding to mix-designs with short fluidity times;
– Fig. 11 presents a part of these lines corresponding to mix-designs with longer fluidity time; and,
– Fig. 6 corresponds to mix-designs with very long fluidity time.

An attempt of schematic representation of the master line trends is given in Fig. 15. To transform the hard paste into a fluid becomes more difficult as the total mixing time is longer. However, this tendency is reversed for the very hard-to-mix concrete in the twin-shaft mixer: the main difficulty becomes to transform the wet granular mixture into a hard paste. It may be supposed that this reversed tendency exists in planetary systems, but no ultra high performance concrete was produced in the present tests in planetary mixer.

6. Conclusion

It is usually considered that the mixing of a concrete mainly consists in i) dispersing the constituents in the mixed volume, and ii) changing the mixture from a wet granular to a granular suspension micro-structure. The constituents' distribution becomes stable in a rather short mixing time (mostly during mixer loading). The microstructure evolution lasts longer.

This paper deals with the microstructure evolution during mixing. It is shown here that five mixture states may be considered: dry powder, dry granules, wet granules, granular suspension including agglomerates and dispersed granular suspension. Agglomerates are defined here as clusters of very fine particles bounded by cohesion forces and/or a hydrate membrane. Granules are larger microstructural elements, made of agglomerates and coarser elements, bonded by liquid bridges. The mixing kinetics mechanism proposed here consists in four mixing-stages: granules growth, granules coalescence, granules dissolution and agglomerates dispersion. The mixing-stages correspond to the mixture transformation following the above presented five successive mixture states.

Basically, the first three mixing-stages of the microstructure evolution are an effect of granules compaction under shearing. Liquid liberated by granules consolidation conducts to their dissolution in the granular suspension state.

Two transition times, the maximum cohesion time and the fluidity time, are defined in this paper. The maximum cohesion time is the transition from the wet granular state to a state where granules not yet dissolved are already connected by liquid bridges (hard paste). The fluidity time is the instant of transition from a hard paste to a granular suspension state in all mixed volume. Beginning with the fluidity time the mixture has already a fresh concrete appearance. In that sense, the fluidity time is considered as an indicator of mixture mixing difficulty for a given mixer.

It is shown that the time evolution of the mixer power consumption is relevant tool to identify the transient stages of the mixture during mixing. A first power peak is associated to the end of constituents' loading and dispersion. A second power peak (if any) corresponds to the maximum cohesion point. The fluidity point is related to a fast attenuation of the power signal fluctuation. For some easy-to-mix mixtures, the fluidity point also corresponds to an angular point on the power curve. For hard-to-mix concrete, the reading of the fluidity point may still be difficult and more research is needed to bring a complete answer for the in-line detection by curve analyses.

Some main trends of the mixing behavior were studied by using three sets of experiments. It seems that the liquid loading into solid components sequence has no significant influence on the mixing behavior after all components loading.

In the power consumption to mixing time chart, both maximum cohesion point and fluidity point are located on master curves which are independent on the mix-design: the maximum cohesion line and the fluidity line, respectively. For the two mixing systems investigated in this paper, twin-shaft and planetary mixer, the fluidity line is mostly bi-linear. The fluidity points are located on the fluidity line in the increasing order of the rheological properties of the mixed concrete at the fluidity point.

Acknowledgments

The presented tests were realized, with different objectives, in a number of joint researches, involving several industrial partners of the Laboratoire Central des Ponts et Chaussées, which are kindly acknowledged: Couvrot group Skako, Béton de France, Liebherr France, Eiffage, Sika, SCC French National Project. The authors particularly thank Eric Brunquet for the very rich discussions on this subject and Michel Dauvergne, David Chopin, Bernard Guieysse, Olivier Garcin, Pierre Chelet, Daniel Michel, François de Larrard, Samuel Masson, Philippe Sloma who carried out or participated to conceive the experimentations.

References

[1] E. Brunquet, B. Cazacliu, In-situ on-line control of SCC production regularity, 5th International Symposium on Self-Compacting Concrete, Ghent, 2007, pp. 251–259.
[2] R. Teillet, S. Bruneaud, Y. Charonnat, Suivi et contrôle de la fabrication des mélanges. Une nouvelle jeunesse pour le wattmètre différentiel, Bulletin de Liaison des Laboratoires des Ponts et Chaussées 174 (1991) 5–16.
[3] Moshe Te'eni, System and method for controlling concrete production, United States Patent 6,227 (039) (May 2001) B1.
[4] K. Wang, J. Hu, Use of a moisture sensor for monitoring the effect of mixing procedure on uniformity of concrete mixtures, Journal of Advanced Concrete Technology 3 (3) (2005) 371–384 2005.
[5] R. Board, On-line moisture measurement by Hydronix, Canadian Ceramics Quarterly 66 (2) (1997) 99–102.
[6] D. Chopin, B. Cazacliu, F. de Larrard, R. Schell, Monitoring of concrete homogenisation with the power consumption curve, Materials & Structures 40 (9) (2007) 897–907.
[7] H. Lombois-Burger, P. Colombet, J.L. Halary, H. Van Damme, Kneading and extrusion of dense polymer–cement pastes, Cement and Concrete Research 36 (2006) 2086–2097.
[8] D.A. Williams, A.W. Saak, H.M. Jennings, The influence of mixing on the rheology of fresh cement paste, Cement and Concrete Research 29 (1999) 1491–1496.
[9] J.P. Jézéquel, V. Collin, Mixing of concrete or mortars: dispersive aspects, Cement and Concrete Research 37 (2007) 1321–1333.

[10] A. Johansson, The relationship between mixing time and type of concrete mixer, Swedish Cement and Concrete Research Institute, Proceedings HANDLINGAR, Stockholm, 1971.
[11] P.-O. Vandanjon, F. De Larrard, B. Dehousse, G. Villain, R. Maillot, P. Laplante, Homogenisation of concrete in a batch plant: the influence of mixing time and method on the introduction of mineral admixtures, Magazine of Concrete Research 55 (2) (2003) 105–116 April.
[12] H. Beitzel, Y. Charonnat, M. Beitzel, Assessment and classification of performance mixers, Materials and Structures 36 (258) (2003) 250–264.
[13] S.M. Iveson, J.D. Litster, K. Hapgood, B.J. Ennis, Nucleation, growth and breakage phenomena in agitated wet granulation processes: a review, Powder Technology 117 (2001) 3–39.
[14] H. Leuenberger, Granulation, new techniques, Pharmaceutica Acta Helvetiae 57 (3) (1982) 73–82.
[15] A. Goldszal, J. Bousquet, Wet agglomeration of powders: from physics toward process optimization, Powder Technology 117 (2001) 221–231.
[16] M. Yang, H.M. Jennings, The influence of mixing methods on the microstructure and rheological behaviour of cement paste, Advanced cement based materials 2 (1995) 70–78.
[17] J.T. Carstensen, T. Lai, D.W. Flickner, H.E. Huber, M.A. Zoglio, Physical aspects of wet granulations 1. Distribution kinetics of water, Journal of Pharmaceutical Sciences 65 (7) (1976) 992–997.
[18] P.C. Knight, T. Instone, J.M.K. Pearson, M.J. Hounslow, An investigation into the kinetics of liquid distribution and growth in high shear mixer agglomeration, Powder Technology 97 (1998) 246–257.
[19] N.O. Lindberg, L. Wenngren, L. Leander, Studies on granulation in a change can mixer, Acta pharmaceutica Suecica 11 (1974) 603–620.
[20] H.P. Bier, H. Leuenberger, H. Sucker, Determination of the uncritical quantity of granulating liquid by power measurements on planetary mixers, Pharmazeutische Industrie 41 (1979) 375–380.
[21] G. Betz, P. Junker Bürgin, H. Leuenberger, Power consumption profile analysis and tensile strength measurements during moist agglomeration process, International journal of pharmaceutics 252 (2003) 11–25.
[22] Leuenberger, New trends in the production of pharmaceutical granules: the classical batch concept and the problem of scale-up, European Journal of Pharmaceutics and Biopharmaceutics 52 (3) (November 2001) 279–288 (10).
[23] S. Watano, T. Tanaka, K. Miyanami, Method for process monitoring and determination of operational end-point by frequency analysis of power consumption in agitation granulation, Advanced Powder Technology 6 (2) (1995) 91–102.
[24] I. Talu, G.I. Tardos, R.J. van Ommen, Use of stress fluctuations to monitor wet granulation of powders, Powder Technology 117 (2001) 149–162.
[25] Loring, Purrington, The determination of the workability of concrete, ASTM 28 (1928) 499 part.II, New Hampshire.
[26] G. Reverdy, Contrôle électrique intégral de la fabrication des bétons hydrauliques, Révue Générale des Routes 381 (10) (1963) 125–126.
[27] P. Delude, R. Ambrosino, Controle en centrale de la quantité d'eau de gâchage du béton, Bulletin de Liaison des Laboratoires des Ponts et Chaussées 16 (1965) I29–I36.
[28] C.h. Parey, J. Durrieu, Les centrales de béton routier — Contrôle en cours de fabrication et contrôle a posteriori, Bulletin de Liaison des Laboratoires des Ponts et Chaussées 30 (1968) 137–158.
[29] M. Champion, V. Zouboff, Utilisation d'un wattmètre différentiel de Bordeaux pour le contrôle d'un poste d'enrobage discontinu, Bulletin de Liaison des Laboratoires des Ponts et Chaussées 34 (1968).
[30] R. Boussion, R. Teillet, Histogrammeur pour wattmètre différentiel, Bulletin de Liaison des Laboratoires des Ponts et Chaussées 60 (1972) 33–38.
[31] Y. Charonnat, Y. Tricart, Enregistrement des paramètres de fabrication sur les centrales à béton, Bulletin de Liaison des Laboratoires des Ponts et Chaussées 48 (1970).
[32] M. Mamillian, J. Simmonnet, Un nouveau dispositif pour régler l'ouvrabilité du béton en cours de malaxage, Le servo-ouvrabilimètre, Annales de l'ITBTP, 270, 1970.
[33] M. Brachet, Y. Charonnat, M. Ray, Vers un contrôle non conventionnel des bétons hydrauliques, Annales de l'ITBPE, suppl. au 336, 1976.
[34] Lichtenberg E.H. Method of and apparatus for determining the consistency of concrete, US patent 1,730,893, patented Oct. 8 1929.
[35] S. Amziane, C. Ferraris, E. Koehler, Measurement of workability of fresh concrete using a mixing truck, Research of the National Institute of Standards and Technology 110 (1) (2005) 55–66.
[36] N. Nishiyama, Controlling the consistency of high-performance concrete by mixing torque in the ready-mixed concrete plant, Proc. 15th Ann. Meeting JCI, 1993, pp. 633–648.
[37] Waitzinger et al., Concrete mixer having means for determining the consistency of concrete mixing therein, United States Patent, 4,900,154, February, 1990.
[38] D. Chopin, F. de Larrard, B. Cazacliu, Why SCC and HPC are so long to mix? Cement and Concrete Research 34 (12) (2004) 2237–2243.
[39] G.H. Tatersall, P.F.G. Banfill, The Rheology of Fresh Concrete, Pitman Advanced Publishing, Boston, 1983.
[40] F. de Larrard, Concrete Mixture Proportioning — A Scientific Approach. Modern Concrete Technology No. 9, E & FN SPON, 1999 441p.
[41] F. de Larrard, C. Hu, T. Sedran, J.C. Sitzkar, M. Joly, F. Claux, F. Derkx, A New Rheometer for Soft-to-Fluid Fresh Concrete, ACI Materials Journal 94 (3) (1997) 234–243.
[42] B. Cazacliu, N.D. Lê, F. de Larrard, New methods for accurate water dosage in concrete central mix plants, Materials and Structures 41 (10) (2008) 1681–1696.
[43] B. Cazacliu, J. Legrand, Characterization of the granular-to-fluid state process during mixing by power evolution in a planetary concrete mixer, Chemical Engineering Science 63 (18) (2008) 4617–4630.
[44] A.B. Metzner, E.R. Otto, Agitation of non-Newtonian fluids, A.I.Ch.E. Journal 3 (1957) 3–10.